Drink. Water Eng. Sci. Discuss., 4, 61–83, 2011
www.drink-water-eng-sci-discuss.net/4/61/2011/
doi:10.5194/dwesd-4-61-2011
© Author(s) 2011. CC Attribution 3.0 License.

Open Access
Drinking Water
Engineering and Science
Discussions

This discussion paper is/has been under review for the journal Drinking Water Engineering and Science (DWES). Please refer to the corresponding final paper in DWES if available.

Experimental investigation of turbulent particle radial transport processes in DWDS using optical tomography

R. Floris and P. van Thienen

KWR Watercycle Research Institute, Groningenhaven 7,
3433 PE Nieuwegein, The Netherlands

Received: 10 May 2011 – Accepted: 21 May 2011 – Published: 6 July 2011

Correspondence to: R. Floris (ro.floris@gmail.com)

Published by Copernicus Publications on behalf of the Delft University of Technology.

Abstract

Several transport mechanisms govern the cross-sectional particle distribution in fully developed turbulent flow in a pipe. These transport mechanisms affect particle load deposition as well as particle resuspension, which are identified as principal protagonists in the build-up of potential discolouration risk in drinking water distribution systems (DWDS). Both are to a large degree controlled by particle size and flow conditions. However, so far, these relationships are not completely understood in the context of DWDS.

In this research we have attempted to identify under which conditions particles suspended in water are transported towards the pipe wall, which generate favourable conditions for deposition. Experimental results are reported and then compared, qualitatively and quantitatively, to the theoretical predictions in the regime transport map for turbulent flow proposed by van Thienen et al. (2011a). The research was conducted by completing a series of experiments in a laboratory test facility with different hydraulic regimes and different particle size ranges. A newly developed optical tomography measurement system was used in order to produce cross-sectional images of particle concentration in water flowing inside a pipe. The experimental results allowed us to identify flow conditions and particles sizes under which gravitational settling and turbophoresis dominated the radial particle transport. These findings show a good correspondence between experimental data and theoretical predictions on the occurrence of turbophoresis and lead to a better understanding of the processes that increase the potential discolouration risk in DWDS.

1 Introduction

The drinking water which is supplied to the customers tap is not the same quality as when it left the treatment plant. In spite of the high quality standards of water produced, globally water companies receive a significant number of complaints relating to

DWESD
4, 61–83, 2011

quality problems (Vreeburg and Boxall, 2007; Husband and Boxall, 2010). Previous research conducted in the last decade has highlighted that several processes, chemical, physical, biological, and hydraulic, affect the water quality during transport through the DWDS. Although in the strict sense of the word it is not a quality problem (no dissolved contaminants), discolouration of water is statistically the first trigger that provokes customers complaints.

Discolouration events show themselves as a change in the appearance or colour of the drinking water due to suspended particles which influence the optical properties of the bulk water. Particles can come into the network directly from the treatment plant and from the DWDS itself by corrosion of iron pipes, flocculation of colloids, precipitation of dissolved elements and as a consequence of biological activity (Slaats et al., 2002; Vreeburg, 2007). Under regular operating conditions, particles tend to settle and accumulate within the network and this can be considered the first step in the generation of discoloured water. The second step is the resuspension of accumulated material that could occur as a result of changes in the prevailing hydraulic regime caused by operating valves, the use of water for fire fighting or any essential maintenance operation on the network. Particle load deposition and resuspension are to a large degree controlled by the flow conditions. Changes in the flow velocity modify the magnitude of the forces acting upon the particles and, as a consequence, affect the transport mechanisms leading to deposition or resuspension. However, so far, these relationships are not completely understood. In this work we focus on radial particle transport as observed from the cross-sectional particle distribution in the pipe, which can be considered the result of the balance between several transport mechanisms and the precursor of particle load deposition. Because DWDS frequently operate under turbulent flow conditions, in addition to gravitational settling (Ryan et al., 2008), turbulent diffusion and turbophoresis play a relevant role and have to be considered in the build-up of discolouration potential (van Thienen et al., 2011a).

Generally computational or experimental results concerning the behaviour of suspended particles in turbulent flow are presented (Fig. 1) as curves of dimensionless

cc BY

deposition velocity versus dimensionless particle relaxation time (see Guha, 1997, 2008; Young and Leeming, 1997). The typical S-shaped curve exhibits three distinct transport regimes: (i) the diffusional deposition regime characterised by turbulent and molecular diffusion processes, (ii) the diffusion impaction regime where the influence of turbulent diffusion is decreased and the influence of turbophoresis is increased, and (iii) the particle inertia moderated regime where the increase of inertia effects generate a reduction in the response of the particles to turbulence (Guha, 1997, 2008; Young and Leeming, 1997). So far, studies have focused on the field of dry particle deposition (Sippola and Nazaroff, 2002; Marchioli et al., 2003; Zhao and Wu, 2006) and only few studies have focused on the effects of turbulent conditions on particles suspended in water (Husband et al., 2008; Ryan et al., 2008).

The objective of the research reported here is to study the flow conditions and particle size for which either gravitational settling, turbulent diffusion or turbophoresis dominate radial particle transport and to verify qualitatively and quantitatively the modelling approach proposed by van Thienen et al. (2011a), an application of the turbulent particle deposition theory of Young and Leeming (1997) and Guha (1997, 2008) to DWDS that includes additional effects and forces relevant for drinking water distribution systems.

2 Theory of radial particle transport

The behaviour of suspended particles during turbulent flow conditions has been studied from several points of view. Interest exists in many fields of research, both engineering and scientific. A common goal of these studies is to identify when deposition occurs and to determine the rate and the velocity of particle deposition. A large number of contributions can be found within literature which have particular reference to the behaviour of particles suspended in air (Sippola and Nazaroff, 2002; Marchioli et al., 2003; Zhao and Wu, 2006). However, only few research projects have been applied to DWDS conditions.

DWESD
4, 61–83, 2011

R. Floris and P. van Thienen

CC BY

Guha (1997, 2008) and Young and Leeming (1997) have presented a theory of particle deposition based formally on the conservation equations of particle mass and momentum for fully developed turbulent flow. Formulating the equations in an Eulerian system and performing Reynolds averaging, they obtained a time-mean particle transport equation in turbulent pipe flow. Through a mathematical derivation these models provide a physical understanding of the various transport processes such as Brownian diffusion, turbulent diffusion, thermophoresis and turbophoresis. If a concentration gradient exists, the macroscopic result of Brownian motion is a net transport of particles towards a region with low concentration resulting in a reduction of the concentration gradient, i.e. in a concentration field homogenization. Turbulent diffusion has the same macroscopic result as the Brownian diffusion. However it is achieved by the turbulent flow eddies. These processes can be modelled together by a modified Fick's law expressing the total diffusion by:

$$J = -(D_\mathrm{B} + D_\mathrm{T})\, \nabla C \tag{1}$$

where D_B is the Brownian diffusivity, D_T is the turbulent diffusivity and ∇C is the concentration gradient. The turbulent diffusion is usually considered several orders of magnitude faster than the Brownian diffusion. Turbophoresis, first identified by Caporaloni et al. (1975), is the particle transport generated by the interaction between inhomogeneity of fluid turbulent flow field and the particle inertia. The particles are led towards regions with lower turbulence intensity. In a fully developed turbulent pipe flow the cross-sectional turbulence intensity distribution is characterised by a radial symmetry because of the boundary layer effects which decay to zero as the turbulence velocity fluctuates. This condition generates a high turbulence intensity gradient, located in the near wall region, with its thickness a function of the bulk flow velocity. The result is a particle flux directed towards the wall, directly proportional to the gradient of turbulence intensity, which increases the cross-sectional concentration gradient.

Young and Leeming as well as Guha recognized turbulent diffusion and turbophoresis as the main mechanisms that cause particle deposition. Both models have been

DWESD
4, 61–83, 2011

CC BY

developed for aerosols and some modifications are required to apply them in the perspective of particles suspended in water. Van Thienen et al. (2011a) have applied the Young and Leeming model to consider the different particle transport and the relative changes in the forces acting and their relative magnitudes. The method considers turbulent transport processes and includes the virtual mass effect (Odar and Hamilton, 1964).

Experimental results or calculations are generally represented as curves of dimensionless deposition velocity versus dimensionless particle relaxation time (Fig. 1). Using the Guha definition, the deposition velocity, V_{dep}, is the particle mass transfer rate in the normal wall direction, J, (mass or number per area per time) normalized by the mean or bulk concentration, C_0, (mass or number per volume) in the pipe flow

$$V_{dep} = \frac{J}{C_0} \tag{2}$$

The particle relaxation time, τ_p, can be considered as a measure of the relative importance of particle inertia and drag forces and represents the time response of the particle to a change in the velocity conditions. It can be calculated by (van Thienen et al., 2011a):

$$\tau_p = \frac{\left(2\,\rho_p + \rho_w\right)\,d_p^2}{36\,\rho_w\,\nu} \tag{3}$$

where ρ_p is the particle material density, d_p is the particle diameter, ρ_w is the fluid density and ν is the kinematic fluid viscosity. Deposition velocity and particle relaxation time are made dimensionless by the fluid friction velocity u^* and the kinematic fluid viscosity. The fluid friction velocity for a fully developed turbulent pipe flow can be determined by considering the bulk flow velocity (Zanoun et al., 2007):

$$\frac{U_b}{u^*} = \frac{1}{k}\ln\left(\frac{R\,u^*}{\nu}\right) - \frac{3}{2\,k} + B \tag{4}$$

cc BY

where k is the Von Kármán constant, R the pipe inner radius, ν the kinematic fluid viscosity and B a dimensionless additive constant. The typical S-shaped curve (Fig. 1) shows that particle transport behaviour can be classified in three regimes: the diffusional deposition regime, the diffusion impaction regime and the particle inertia moderated regime. The diffusional deposition regime is mainly governed by Brownian and turbulent diffusion. According to the modified Fick's law, the deposition velocity reduces proportionately with τ^+ as a result of a decrease in the turbulent diffusivity as the particle diameter increases. In the eddy diffusion-impaction regime, the deposition velocity increases by several orders of magnitude. This regime is characterized by a high response of particles to the turbulence of the flow. In the inertia-moderate regime the deposition velocity slight decreases turbophoretic effects decrease because the particle inertia increases.

Using the expressions Eqs. (3) and (4) van Thienen et al. (2011a) have theoretically determined the range of conditions relevant for drinking water distribution systems in which different radial particle transport mechanisms can be expected to operate as function of bulk flow velocity U_b and particle diameter (Fig. 2). Both turbophoresis and turbulent diffusion can be expected to affect radial particle movement in drinking water distribution pipes. Turbulent diffusion is more relevant for small particle diameter and low velocity whereas turbophoresis plays as significant role at high velocity and large particle diameter. These results are qualitatively supported by lab experiments (Vreeburg and Boxall, 2007) in which water containing hydroxide flocs was re-circulated through a perspex pipe loop. The experiments showed two different modes of deposition into a pipe (see Fig. 3): at low flow velocity ($0.06\,\mathrm{m\,s^{-1}}$) the iron hydroxide flocs settle only in the bottom half of the pipe whereas at high flow velocity ($0.14\,\mathrm{m\,s^{-1}}$) the deposition of the flocs occurs all around the inner surface of the pipe, including the upper half. Plotting the values of the flow velocity and the range of the iron hydroxide flocs size (100–1000 µm) in the graph proposed by van Thienen et al. (2011a) the first mode of sedimentation can be qualitatively assigned to the diffusion dominated regime and the second to the inertia-moderate regime where turbophoresis leads particles towards

DWESD
4, 61–83, 2011

R. Floris and P. van Thienen

the wall of the pipe.

3 Experimental test rig

The experiments were carried out using a test facility at the KWR laboratory which has been built to investigate sediment transportation and the process by which material is lost from the bulk fluid to the pipe wall under conditions similar to those in a DWDS. The main elements of the test rig are: a tank, a vertical pump with variable flow control, a digital flow meter, 2 transparent perspex pipes, through which water with sediment flows, and an optical tomography measurement system (Fig. 4). In order to approximate a normal distribution pipe as much as possible the main pipe section has two parts with inner diameters of 81 mm and 101 mm respectively. Both have an inlet structure and a length of approximately 2 m, to allow the flow to stabilize after bends, valves and joints. In order to minimise sedimentation outside the perspex pipe section, the rest of pipe loop was designed with a smaller inner diameter allowing flow velocities of three to five times those of the monitoring pipes. Therefore the wall shear stress should be high enough to prevent the sediment particles settling within the pipe. Because of the large amount of particles contained in the tank it is possible to keep the particle concentration almost constant during the experiments. Considering the allowable size of solids pumped (5 µm to 1 mm) and the maximum velocity achievable in the monitoring pipe (1.1 $m\,s^{-1}$) the test rig allowed us to simulate most typical conditions found in a DWDS. Certain specific flow patterns are not detectable by visual observations through the transparent pipes alone. To solve this problem and to better understand the cross-sectional particle distribution, a new optical tomography measurement system has been used.

DWESD
4, 61–83, 2011

Discussion Paper | Discussion Paper | Discussion Paper | Discussion Paper |

4 Optical tomography

Tomography is a non-invasive technique of imaging that allows the study of the internal structures of an object or a system without influence or conditioning it. Mainly used in the field of medicine, tomography has been also applied in industry (non-destructive testing) and science (3-D imaging of nanomaterials) in the last decades (Dyakowski et al., 2000; Fokeer et al., 2004; Zheng et al., 2006). Several types of tomography techniques are available (seismic tomography, electrical capacitance tomography, electrical resistance tomography, electrical magnetic tomography, optical tomography, X-ray, γ-ray, etc...). The common basic principle of these techniques is to analyze the interaction between the system studied and a physical field and then to translate this information into images of the system being studied. Here an optical tomography technique was used to enable different particle concentration fields using the interaction between light and particles suspended in flowing water. A full description of the methodology is given in van Thienen et al. (2011b). Here, we give a brief outline.

On passing through a turbid fluid, the beam of light is in part scattered and in part absorbed as a function of the fluid turbidity. In other words, there is a relationship between the optical property of the fluid and the suspended particle concentration that constitutes the turbidity. Analysing the variations in the light intensity field, it is therefore possible to obtain the concentration distribution throughout the cross-section.

The optical tomography measurement system comprises an optical tomography device (OTD) and an Arduino microcontroller board connected to the device and to a workstation. The OTD generates light pulses from 10 high power light emitting diodes (LED) and detects the interaction between these pulses and the suspension using 10 light sensors (LS). The LEDs and the LSs are installed alternatively in a PVC ring that surrounds the monitoring pipe and they are controlled by the Arduino board (Arduino, 2010) on which is installed custom made control software. The LEDs are operated sequentially and for every light pulse data are collected by every LS. In this way it is possible to investigate the concentration field using 100 light beams within every measurement cycle. The data collected are transmitted at the workstation which computes a tomogram of the light absorption coefficient field by an inverse problem algorithm. The tomogram is a 2-D image representing the variation of the light absorption coefficient representative of the local particle concentration through a cross-section of the suspension flow.

5 Experimental setup

To investigate the transport of particles towards the wall, in the present application, we performed several experiments re-circulating a suspension of particles in clean water through the test rig described in Sect. 3. These particles may be sand, kaolinite, sediment from a distribution system, or iron hydroxide flocs formed by dosing with iron chloride. Used coffee granules (i.e. those from which soluble substances have already been extracted in the process of making coffee) were chosen because of three factors; their density (900–1100 kg m^{-3}) is close to the density of sediment samples collected from DWDSs (Boxall et al., 2001), their optical properties (high light absorption and low light reflection) and their physical and chemical stability after extraction. As a further matter coffee particles do not bond to the inner pipe surface, i.e. they do not change the pipe roughness during the experiment, which would significantly enhance deposition (Guha, 2008) and do not change the optical proprieties of the perspex pipe wall. Moreover, this material is easy to sieve in several particle size ranges.

We performed a parameter space search for particle size and flow velocity. Changes in the flow pattern (cross-sectional particles distribution) as a function of the flow conditions were observed. For each experiment a coffee suspension in clean water characterized by a bounded particle size range was circulated through the pipes. The flow conditions were changed by increasing or decreasing the flow velocity with 0.05 m s^{-1} steps using a variable frequency drive installed on the pump in combination with a throttle valve. The bulk flow velocity range started at a value 0.1 m s^{-1} and then increased

CC BY

up to 1.1 m s^{-1}. The particle size ranges used in these experiments are reported in Table 1.

The optical tomography device was located at the end of the second transparent pipe to ensure that the flow could reach steady conditions after the bends. As explained in Sect. 4, the tomogram images obtained are the result of an inverse problem where the inputs are the light intensities collected during a measurement cycle. Every measurement cycle took less than 1 s to acquire a complete intensity light data set. For each LED-Sensor combination, 19 samples were taken. Both averages and standard deviations were used as input for the inversion procedure (see van Thienen et al., 2011b). This approach allowed us to average out the random variations in concentrations and obtain more stable tomograms. These do not represent snapshots but average conditions of the particular cross-section, taken over a period of time (<1 s) under steady flow conditions. The tests were conducted at constant water temperature and shielding of the investigation section from the external light.

6 Results

Changes in the flow pattern in relation to the bulk flow velocity variations present the same trend in all of the experiments conducted with large particles (>425 µm). Figure 5 summarizes the occurrences of different flow patterns relative to 4 several bulk flow velocities of a coffee particle suspension (particle size ~500 µm) in steady conditions. Up to a bulk flow velocity of 0.25 m s^{-1} (Fig. 5a–c), a large fraction of the particles is located at the bottom of the pipe moving as bed transport load. Increasing the bulk flow velocity to 0.50 m s^{-1} (Fig. 5d–f), the structure of the flow becomes unstable and in the tomogram an annulus of high particle concentration is visible in the lower part of the pipe. This annulus grows with increasing the bulk flow velocity. This flow pattern is in fact an intermediate between the bed transport and a fully ring-shaped pattern. In the transition regime the tomogram is unstable and changes continuously but always from a more or less extended annular flow pattern. Above of 0.75 m s^{-1}

DWESD
4, 61–83, 2011

(Fig. 4g–i), the tomogram shows a complete ring-shaped flow pattern, thicker at the bottom than the top and with a low particle concentration in the core of the pipe flow. The averaged tomograms also show an axial symmetry. The experiments conducted with smaller particles (<365 µm) do not show the intermediate transport regime but for velocity higher than 0.21 $\mathrm{m\,s^{-1}}$ the transition occurs directly to the ring-shaped flow pattern.

The transition velocities observed during the experiments performed are reported in Fig. 6 which also displays the model predictions discussed in Sect. 2. For particle sizes smaller than 365 µm, the first flow pattern change occurs at 0.21 $\mathrm{m\,s^{-1}}$ and for particle size bigger than 425 µm at 0.35 ± 0.4 $\mathrm{m\,s^{-1}}$. For particle size bigger than 425 µm only, the velocity at which it is possible to observe a complete ring of high concentration increases with increasing particle size.

7 Discussion

Several transport mechanisms govern the cross-sectional particle distribution in drinking water distribution networks. These transport mechanisms are largely controlled by particle size and flow conditions and predictions relating to the transport regimes have been proposed by van Thienen et al. (2011a). We have performed a parameter space search for particle size and flow velocity in order to verify these model predictions. For all of the experiments the transition to turbophoresis dominated patterns takes place in a range of conditions predicted from theory. At low velocity the radial particle transport is governed by gravitational forces and the particles suspended tend to deposit on the bottom of the pipe, moving as bed transport load. Increasing the flow velocity particles at first are re-suspended from the bottom of the pipe and then, under the influence of turbophoresis, they are carried towards the pipe wall generating a ring of high particle concentration through the pipe cross-section. This transition between the bed transport and the ring flow pattern occurs for particles with dimension smaller than 365 µm whereas for particles with dimension larger than 425 µm, the transition occurs through an intermediate flow pattern characterized by an annulus of high particle concentration located in the bottom half of the pipe. The annulus extent increases with the flow velocity until the annulus itself becomes a ring. The velocity at which this second transition in the flow pattern occurs is directly related to the dimension of the suspended particles.

Although a good correspondence between model predictions and experimental results was obtained in the location of the turbophoresis regime, the observed boundary of the turbophoresis dominated regime in Fig. 6 does not correspond to the theoretical boundary in terms of slope. These differences could be explained considering that theoretical boundaries are calculated for the transition between turbulent diffusion and turbophoresis regime and here we seem to observe the transition between gravitational forces and turbophoresis dominated patterns. Turbulent diffusion effects are not evident in these results. The bed transport tomograms slightly diverge from the actual situation in the pipe in thickness and shape of the high particle concentration zone. This resolvability inaccuracy results from resolution issues and possible smearing effects in the inversion procedure. Note that the tomograms show minimum values for the light absorption coefficient which are actually below zero. Obviously, this is not physically meaningful. It results from the fact that the inversion procedure takes into account the uncertainties in input values and from these computes the variance of the solution. The tomogram actually shows the mean image which can be reconstructed, but the fact that with these mean values a variance is associated which shows the actual spread of acceptable values for a specific part of the solution should be kept in mind. A node showing a negative value may therefore still have a significant likelihood of actually being a non-zero value. For more details, the reader is referred to van Thienen et al. (2011b).

The findings are satisfactory to warrant further research into the conditions in which gravity effects and turbophoresis forces govern the cross-section particle distribution but the validation of the model predictions can not be considered complete because of the lack of data in the region that could be largely governed by turbulent diffusion (particle size smaller than 100 µm).

DWESD
4, 61–83, 2011

This research has attempted to identify under which conditions particles suspended in water are transported towards the wall generating favourable conditions for the sedimentation process. These findings move towards a better understanding of the dominant processes that cause particle deposition and therefore increase potential discolouration risk. They could be useful to provide guidance to engineers in respect of understanding system performance and required maintenance to reduce the occurrence of discolouration events. The approach outlined in this study might be replicated with other materials and other particle size range in order to acquire a larger data collection and to generate a more detailed flow pattern map.

8 Conclusions

This paper presents the first application of the optical tomography technique for radial particle transport in drinking water distribution networks. At low velocities the radial particle transport is governed by gravitational forces and the suspended particles move as bed transport load at the bottom of the pipe. At high flow velocities particles are carried towards the pipe wall under the influence of turbophoresis generating a ring of high particle concentration through the pipe cross-section. These two flow patterns are observed for all the particle class range analyzed. In addition, a transition flow pattern was only observed for larger particles.

Acknowledgements. The authors would like to thank Sidney Meijering and Harry van Wegen for the technical support in the laboratory and the constructive comments and Melanie Tankerville for reviewing the English of this paper. Roberto Floris gratefully acknowledges the Master and Back foundation programme of Regione Sardegna for the grant and expresses personal thanks to Rebecca Townsend.

References

Arduino: http://www.arduino.cc, last access: 6 December, 2010.

Boxall, J., Skipworth, P., and Saul, A.: A novel approach to modelling sediment movement in distribution mains based on particle characteristics, Water Softw. Syst., 1, 263–273, 2001.

Caporaloni, M., Tampieri, F., Trombetti, F., and Vittori, O.: Transfer of particles in nonisotropic air turbulence, J. Atmos. Sci., 32, 565–568, 1975.

Dyakowski, T. Jeanmeure, L. F. C., and Jaworski, A.: Applications of electrical tomography for gas-solids and liquid-solids flows – a review, Powder Technol., 112, 174–192, 2000.

Fokeer, S., Kingman, S., Lowndes, I., and Reynolds, A.: Characterisation of the cross sectional particle concentration distribution in horizontal dilute flow conveying – a review, Chem. Eng. Process., 43(6), 677–691, 2004.

Guha, A.: A unified Eulerian theory of turbulent deposition to smooth and rough surfaces, J. Aerosol Sci., 28(8), 1517–1537, 1997.

Guha, A.: Transport and deposition of particles in turbulent and laminar flow, Ann. Rev. Fluid Mech., 40, 311–341, 2008.

Husband, P. and Boxall, J.: Asset deterioration and discolouration in water distribution systems, Water Res., 45(1), 113–124, 2010.

Husband, P., Boxall, J., and Saul, A.: Laboratory studies investigating the processes leading to discolouration in water distribution networks, Water Res., 42(16), 4309–4318, 2008.

Marchioli, C., Giusti, A., Salvetti, M., and Soldati, A.: Direct numerical simulation of particle wall transfer and deposition in upward turbulent pipe flow, Int. J. Multiphas. Flow, 29(6), 1017–1038, 2003.

Odar, F. and Hamilton, W.: Forces on a sphere accelerating in a viscous fluid, J. Fluid Mech., 18(2), 302–314, 1964.

Ryan, G., Mathes, M., Haylock, G., Jayaratne, A., Wu, J., Noui-Mehidi, N., Grainger, C., and Nguyen, B. V.: Particles in water distribution systems. Technical Report 33, Cooperative Research Centre for Water Quality and Treatment, 2008.

Sippola, M. R. and Nazaroff, W. W.: Particle deposition from turbulent flow: Review of published research and its applicability to ventilation ducts in commercial buildings, Tech. Rep. LBNL-51432, Lawrence Berkeley National Laboratory, 2002.

DWESD
4, 61–83, 2011

R. Floris and
P. van Thienen

CC BY

Slaats, P. G. G., Rosenthal, L. P. M., Sieger, W. G., van den Boomen, M., Beuken, R. H. S., and Vreeburg, J. H. G.: Processes involved in generation of discoloured water, Report No. KOA 02.058, American Water Works Association Research Foundation/Kiwa, The Netherlands, 2002.

van Thienen, P. and Vreeburg, J.: Turbulent processes in drinking water distribution, 12th Annual Water Distribution Systems Analysis conference, Tucson, AZ, September, 2010.

van Thienen, P., Vreeburg, J. H., and Blokker, E. J.: Radial transport processes as a precursor to particle deposition in drinking water distribution systems, Water Res., 45(4), 1807–1817, 2011a.

van Thienen, P., Floris, R., and Meijering, S.: Application of optical tomography to the study of discolouration in drinking water distribution systems, Drink. Water Eng. Sci., in review, 2011b.

Vreeburg, J.: Discolouration in drinking water systems: a particular approach, PhD thesis, Delft University of Technology, 2007.

Vreeburg, J. and Boxall, J.: Discolouration in potable water distribution systems: A review, Water Res., 41, 519–529, 2007.

Young, J. and Leeming, A.: A theory of particle deposition in turbulent pipe flow, J. Fluid Mech., 340, 129–159, 1997.

Zanoun, S., Durst, F., Bayoumy, O., and Al-Salaymeh, A.: Wall skin friction and mean velocity profiles for fully developed turbulent pipe flows, Exp. Therm. Fluid Sci. 32, 249–261, 2007.

Zhao, B. and Wu, J.: Modeling particle deposition from fully developed turbulent flow in ventilation duct, Atmos. Environ., 40(3), 457–466, 2006.

Zheng, Y., Liu, Q., Li, Y., and Gindy, N.: Investigation on concentration distribution and mass flow rate measurement for gravity chute conveyor by optical tomography system, Measurement, 39(7), 643–654, 2006.

Table 1. Size classes of the coffee particles.

	Minimum size [µm]	Maximum size [µm]
1	180	250
2	250	300
3	300	365
4	425	500
5	500	600
6	600	710

DWESD
4, 61–83, 2011

R. Floris and P. van Thienen

CC BY

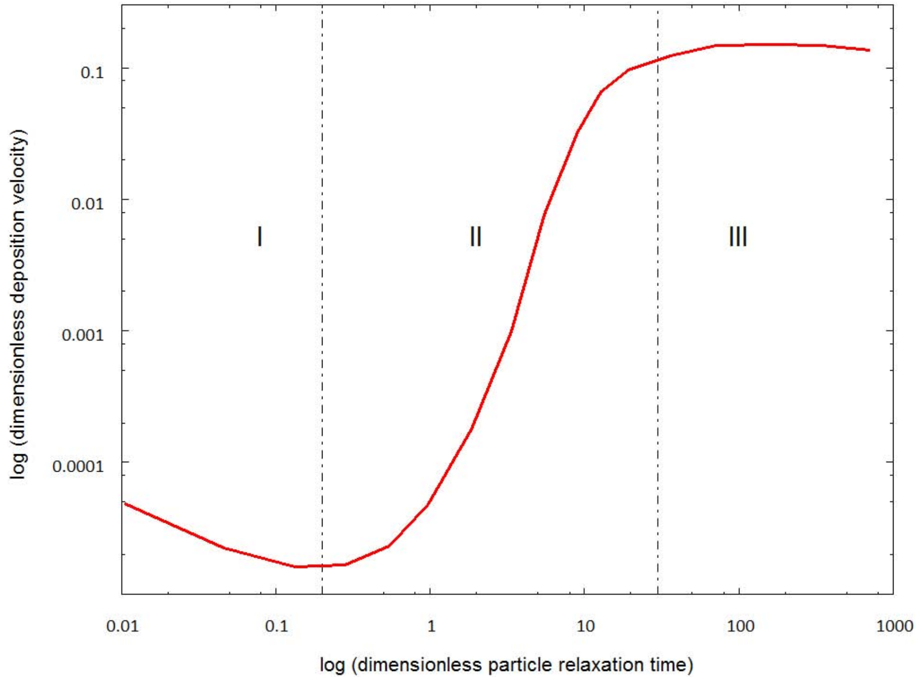

Fig. 1. The typical S-shaped curve of dimensionless deposition velocity V_d^* versus dimensionless particle relaxation time τ_p^*.

DWESD
4, 61–83, 2011

cc BY

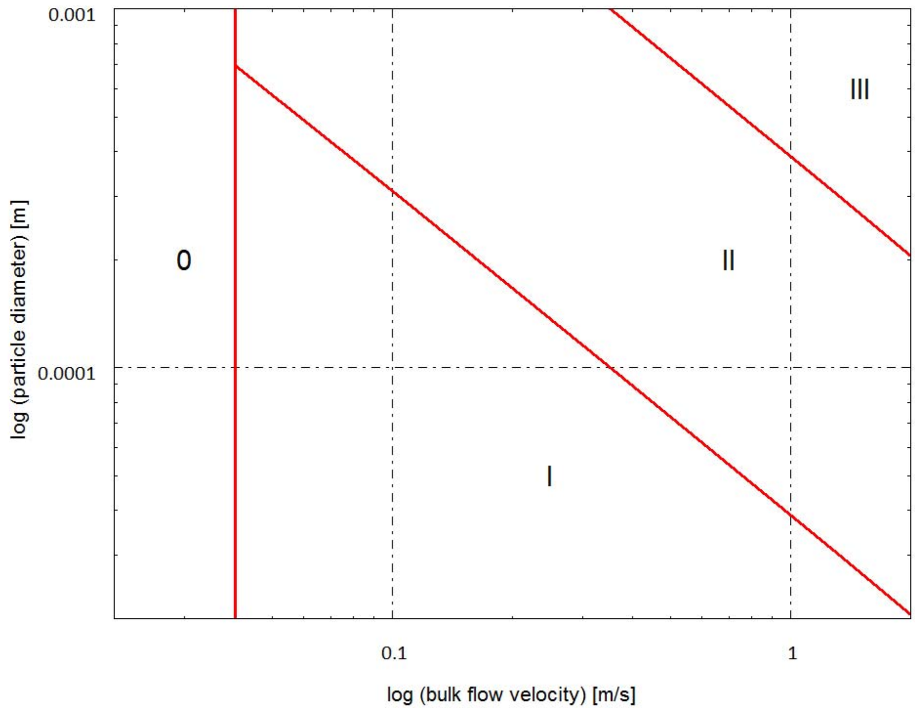

Fig. 2. Radial particle transport regimes as a function of bulk flow velocity U_b and the particle diameter d_m, for a pipe diameter of 100 mm and a particle density of 1.2 g cm^{-3} (from van Thienen et al., 2011a).

DWESD
4, 61–83, 2011

Fig. 3. Hydroxide floc deposition after re-circulation through a perspex pipe loop (inner diameter 100 mm). **(a)** At low flow velocity ($0.06\,m\,s^{-1}$) the iron hydroxide flocs settle only in the bottom half of the pipe. **(b)** At high flow velocity ($0.14\,m\,s^{-1}$) floc deposition occurs all around the inner surface of the pipe. These are the results of a repeat of the original experiment by Vreeburg and Boxall (2007), mirroring their results.

DWESD
4, 61–83, 2011

R. Floris and
P. van Thienen

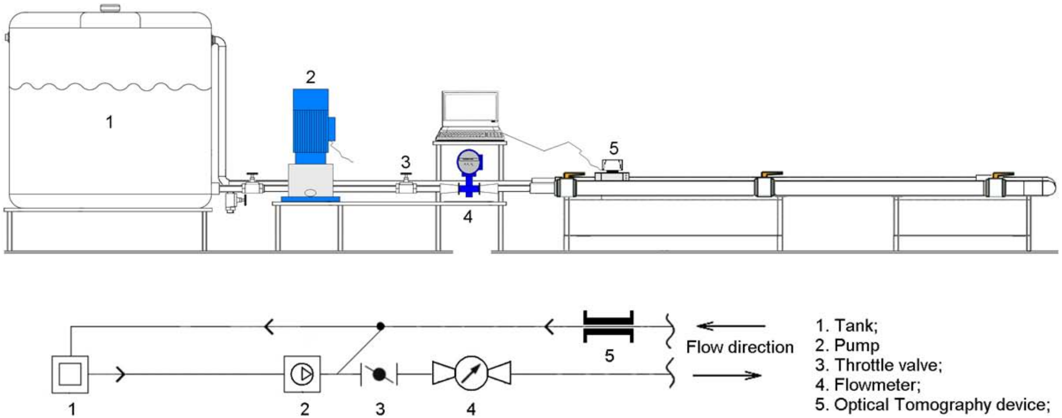

Fig. 4. Schematic description of the experimental test rig.

DWESD
4, 61–83, 2011

Particle radial transport processes in DWDS

R. Floris and
P. van Thienen

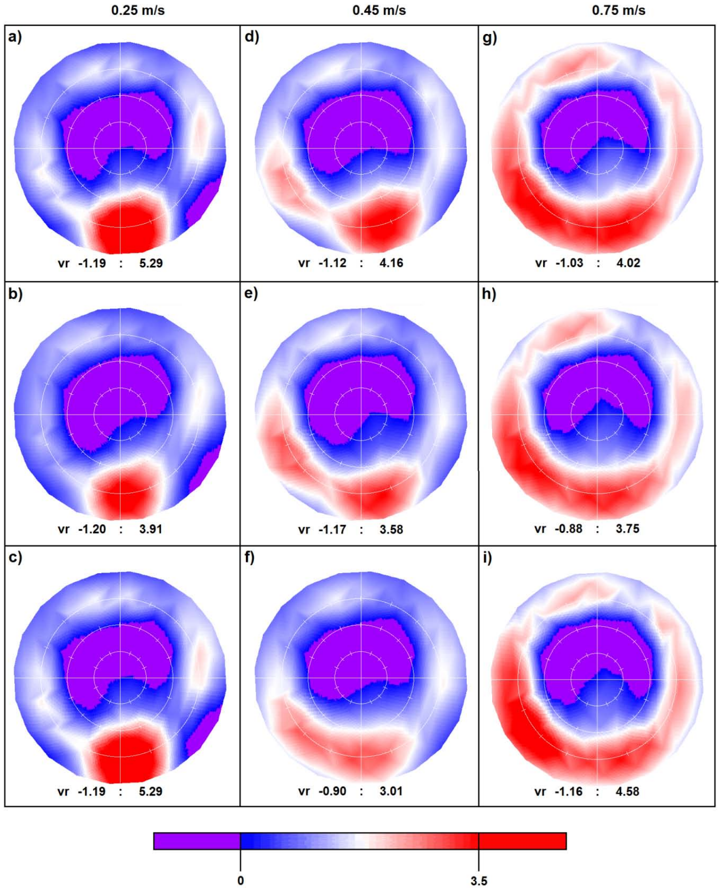

Fig. 5. Different flow patterns of a suspension of water with coffee particles (size ~550 µm), in steady conditions with the respective value range (vr): **(a)–(c)** Bed transport flow pattern at 0.25 $m\,s^{-1}$; **(d)–(f)** annulus flow pattern at 0.45 $m\,s^{-1}$; **(g)–(i)** Ring-shaped flow pattern at 0.75 $m\,s^{-1}$.

DWESD
4, 61–83, 2011

R. Floris and
P. van Thienen

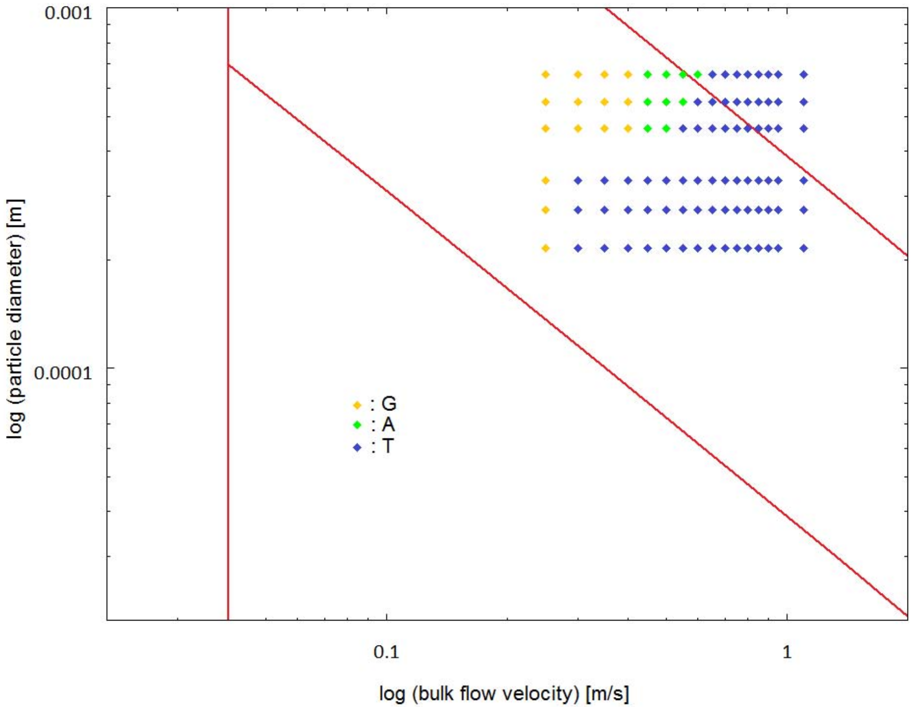

Fig. 6. Location of the experimental data points on the radial particle transport regime map discussed in Sect. 2. G: Bed transport flow pattern; A: Annulus flow pattern; T: Ring-shaped flow pattern.

DWESD
4, 61–83, 2011